RSC Advances

ROYAL SOCIETY OF CHEMISTRY

www.rsc.org/advances

RSC Advances

RSCPublishing

REVIEW

Diagnosis on the measurement inconsistencies of carbon-based electrocatalysts for oxygen reduction reaction in alkaline media

Cite this: DOI: 10.1039/x0xx00000x

Received 00th January 2012,
Accepted 00th January 2012

DOI: 10.1039/x0xx00000x

www.rsc.org/

Dongyoon Shin,[† a] Beomgyun Jeong,[†,b] Myounghoon Choun,[a] Joey D. Ocon,[a] and Jaeyoung Lee[a,b,*]

Finding inexpensive alternative catalysts for the oxygen reduction reaction (ORR) is considered as one of the most overriding challenges in the development of electrochemical technologies. Although significant progress has been made in developing carbon-based ORR catalysts, there is difficulty in judging improvements in the catalysts due to the inconsistent results arising from differences in experimental condition. In this review, we provide a diagnosis on the influence of key factors in the measured ORR activity of catalysts. Knowing the right condition when measuring ORR activity is of paramount importance in establishing a reference for relevant comparison of ORR performance in developed catalysts.

1. Introduction

Oxygen is an ubiquitous electron-accepting agent in a large number of electrochemical technologies and processes.[1–3] In particular, oxygen has a crucial role in the operation of fuel cells and metal-air batteries, which have been gaining traction in the past decades as non-polluting alternative energy sources with high energy densities.[2–5] In these applications, oxygen is converted to water at the cathode *via* the oxygen reduction reaction (ORR) with two possible reaction routes: the direct four-electron pathway and the two-stage pathway with two electrons transferred in each stage and a peroxide intermediate (Scheme 1).

Electrocatalysts facilitate the ORR to have high current densities at potentials as close as possible to the equilibrium potential and selectively *via* the four-electron pathway without formation of corrosive hydrogen peroxide.[6,7] Nevertheless, ORR is kinetically sluggish even in the four-electron route, lowering the overall performance of electrochemical cells.[1,2] With this formidable challenge, there is a concerted effort in the electrochemistry community to synthesize and test new ORR catalysts having superb turnover rates, which will be key in the massive commercialization of electrochemical energy conversion and storage technologies.

Since Döbereiner's discovery of the heterogeneous catalysis of oxygen on platinum (Pt) and Grove's invention of the earliest H_2-O_2 cell using a Pt catalyst for both oxygen reduction and hydrogen oxidation reactions, Pt-based catalysts (Pt black, carbon-supported Pt) have been, indisputably, the best catalysts for ORR.[2,8] The intrinsically high cost of Pt, however, is a serious roadblock in the large-scale roll-out of ORR-involving technologies since the catalyst (i.e. Pt) usually accounts to around 14 % of the total cost.[9] This has led to a very high interest for inexpensive alternative catalysts to Pt (e.g. carbon and non-noble transition metals) that were initially introduced as either a supporting material or as an alloying element to reduce the usage of Pt.[10–14] In addition, another popular approach to increase the activity while at the same time reduce the amount of Pt, is the engineering of catalysts or supported catalysts with specific nano-architectures (i.e. core-shell catalysts, nano-structured thin-film electrodes).[15–18]

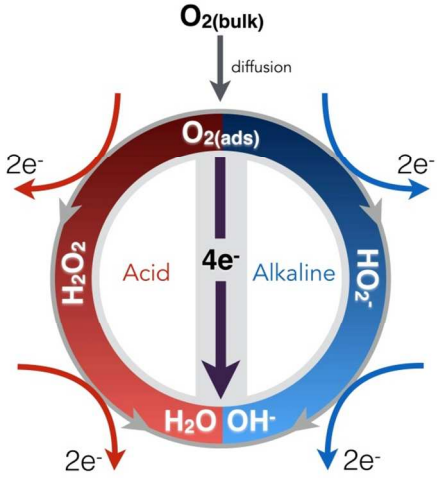

Scheme 1. Reaction pathways of oxygen reduction in both acid (red) and alkaline electrolytes (blue).[1,2]

Although Pt-based catalysts are widely regarded as the best catalysts for ORR at present, they also suffer from technical drawbacks.[7,19] Therefore, there has been a steady movement on the use of Pt-free ORR catalyst in the past decades. Among the alternative non-noble ORR catalysts, pyrolyzed transition metal and heteroatom-modified carbon catalysts have shown huge potential to substitute noble metal catalysts for commercial utilization, with comparable performance even with Pt-based catalyst in both alkaline and acid conditions (Figure 1a).[20,21] An examination of the voluminous literature on metal and heteroatom-modified carbon catalysts would show that its development is akin to mixing the different colors in the color plate on a chosen functionalized carbon material, leading to different ORR-active combinations.[2,7,20,22–27] As shown in Figure 1b, the left-hand side colors represent the transition metals, i.e. manganese (Mn),[28] iron (Fe),[29–33] cobalt (Co),[6,34] nickel (Ni),[35] and copper (Cu),[36] while the right-hand side colors constitute the heteroatom dopants, i.e. boron (B),[37] nitrogen (N),[38–40] phosphorus (P),[41,42] sulfur (S),[43] and selenium (Se),[44] which have been used to modify the catalytic properties of various carbon materials, i.e. graphene, carbon nanotube (CNT), fullerene, diamond, and amorphous carbon.

To further illustrate the analogy above, Co oxide nanocrystals on N-doped graphene have been reported to have excellent ORR activity, arising from the synergism between components[45] and Fe-encapsulated N-doped CNT also shows comparable activity with outstanding stability[31]. Additionally, recent studies have successfully formulated metal-free functionalized carbon materials (e.g. CNT, graphene) that exhibit impressive catalytic activities, even comparable with Pt catalysts.[7,38–41,46,47] Fundamental studies have also been conducted to investigate the reason why metal-free heteroatom doped carbon catalysts demonstrate comparable activity with Pt.[6,48–51]

Of late, a lot of reviews on carbon-based ORR electrocatalysts covering transition metal-carbon complex and metal-free heteroatom-doped carbon have appeared,[3,7,20,52–55] Although significant progress has been made in the development of carbon-based ORR catalysts, differences in experimental condition make it difficult to compare the activities of newly developed catalysts vis-à-vis with other ORR catalysts, as there is a wide variability of the ORR activities within the ORR literature even with Pt catalysts (Figure 1a).[20,21] Thus, this problem needs to be resolved by investigating the effect of various experimental parameters on the performance of carbon-based ORR catalysts. However, a review on ORR with particular emphasis on the key factors affecting this process has never been done before. In the context of making a critical appraisal of the reports on the performance of ORR catalysts, we will discuss the influence of a couple of crucial parameters (e.g. oxygen concentration, non-ORR current, scan direction, catalyst loading) by comparing a family of ORR catalysts from selected publications over the past decades. This review will serve as a handy reference for future researches by establishing a standard ORR activity and as a guide for scientists, especially for non-electrochemists, working on energy conversion and storage.

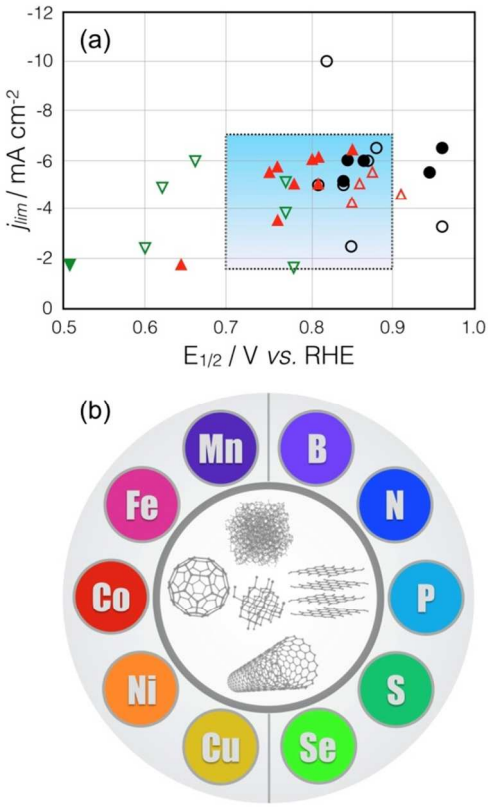

Figure 1. (a) ORR activity comparison of selected electrocatalysts in literature: non-noble metal catalysts (△), metal-free catalysts (▽), and Pt/C catalysts (○) in acid (closed symbol) and alkaline (open symbol) electrolytes. The highlighted rectangular area indicates the reasonable range of limiting currents and half-wave potentials.[20,21] (b) A color plate representing the various transition metals (left side) and heteroatom dopants (right side) that are used to modify the various carbon materials (center).[2,7]

2. Diffusion limiting current and oxygen reduction mechanism

2.1 Inconsistent limiting current depending on oxygen concentration

In electrochemistry, the diffusion limiting current represents the limiting value of the faradaic current due to mass transfer limitations between the electrode surface and bulk of the electrolyte.[56] Levich equation (Eqs. (1), (2)) describes the parameters affecting the magnitude of limiting current.

$$J_L = B\omega^{1/2} \quad (1)$$

$$\mathrm{B} = 0.62 n_e \mathrm{F} C D^{2/3} \upsilon^{-1/6} \quad (2)$$

where B is the Levich slope, ω is the electrode rotation rate, n_e is the number of electron transferred in oxygen reduction reaction, F is the Faraday's constant, C is the oxygen concentration, D is the diffusion coefficient of the dissolved oxygen and υ is the kinematic viscosity of the electrolyte. Typically, the parameter values of F, D, ν are borrowed from

existing literature and C is determined by the experimental condition and ω is a variable controllable with RDE.

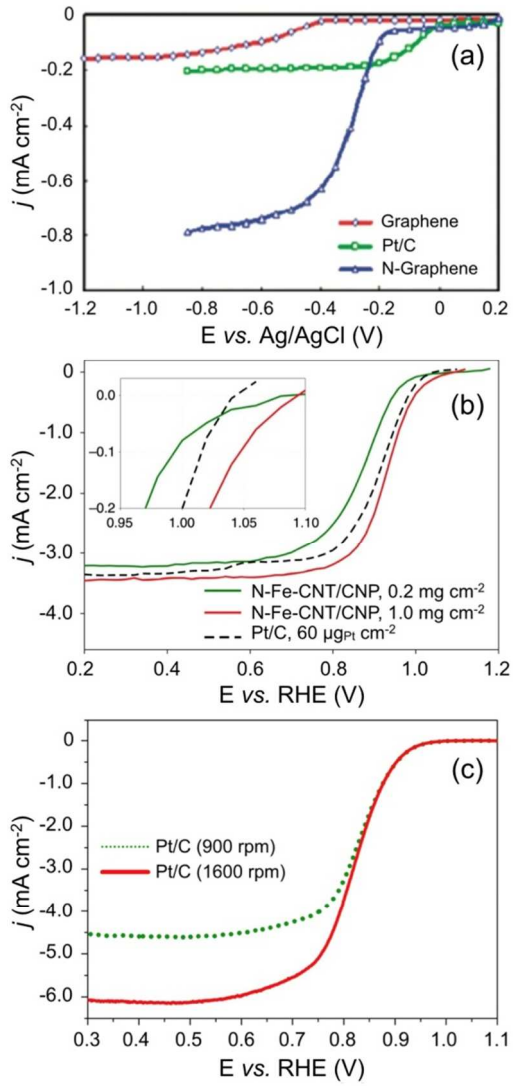

Figure 2. Inconsistent ORR reference performance at different measurement conditions: (a) Rotating ring-disk electrode (RRDE) voltammograms for the ORR in air-saturated 0.1 M KOH with a rotating rate of 1000 rpm and a scan rate of 0.01 V s^{-1} (reprinted with permission from ref. 38 Copyright 2010 American Chemical Society). (b) Steady-state RDE polarization plots obtained using a 20 mV potential step and 25 s potential hold time at every step, with a rotation rate of 900 rpm in O_2-saturated 0.1 M NaOH (25 °C). The inset displays the low overpotential region (adapted by permission from Macmillan Publishers Ltd: Nature Communication (Ref.57), copyright 2013). (c) LSV in a glassy carbon (GC) RDE with 20 wt% Pt/C at a scan rate of 10 mV s^{-1} in O_2-saturated 0.1 M KOH electrolyte.[57,58]

Diffusion limiting current is a good indication of the experimental condition for ORR activity evaluation of catalysts, since it is independent of the applied potential over a finite range and is affected by parameters, which usually are fixed or controlled in the experiment. For example, rotating disk electrode (RDE) is usually used in order to uniformly control the mass transfer by regulating ω during experiments. Thus, the difference in the limiting current between measurements means the existence of several unaccounted factors affecting the ORR activity measurement. As shown in Figure 2, the ORR activities of the commonly used reference catalyst, Pt/C, show a wide difference depending on the experimental condition.[38,47,57–59] The limiting current of Pt/C in Figure 2a shows a much lower than that in Figure 2b, even though the electrode rotating speed is faster in the latter. This difference could have been influenced by oxygen concentration in bulk electrolyte and impurity such as halide anions from the reference electrode (RE).

The diffusion limiting current generally rises with the oxygen concentration in the electrolyte, due to the increase in the number of reactant molecules, until a saturation condition is reached.[60–62] The activity of Pt/C in Figure 2a, which was measured in air-saturated electrolyte, shows a big difference in comparison with other results obtained under the same experimental condition.[38] In addition, the limiting currents in Figure 2b and 2c are slightly different each other, arising from the difference in atmospheric pressure by altitude where the experiments were conducted. In the case of Figure 2b, the results were obtained at Los Alamos in New Mexico, which has a high altitude at over 1,500 m above sea level. Meanwhile, the altitude above sea level is almost 0 m in the case of Figure 2c, which can be quantitatively identified with the Henry's law and the known atmospheric pressure at different altitudes. The observations above suggest that the oxygen amount in air, atmospheric pressure, and electrolyte temperature, all of which affect the oxygen concentration dissolved in the electrolyte, should be considered during ORR performance evaluation for a consistent limiting current density.

The presence of halide anion impurities in the supporting electrolyte dramatically affects not only the kinetics of the electrocatalytic reaction but also the diffusion limiting current on Pt.[63–65] This phenomenon usually occurs because the halide anions, e.g. Cl^-, Br^-, compete with oxygen to cover the free adsorption sites on the catalyst's surface. The ion-modified surface affects the ORR activity of the catalyst and changes the oxygen reduction pathway from direct four-electron pathway to the less-efficient two-electron route. Chloride-containing REs, such as silver-silver chloride (Ag/AgCl) and saturated calomel electrode (SCE), are often used to evaluate ORR activity. There is, however, potential contamination by the Cl^- ions eluted from the saturated KCl solution in the REs, which is a concern for correct measurements on the newly developed catalysts and Pt/C reference catalyst. Moreover, if Ag/AgCl electrodes are in highly alkaline solution for a long time, AgCl could be converted to Ag_xO, which causes the gradual shift of RE potential in positive direction by the mixed potential of Ag/AgCl and Ag/Ag_xO interfaces.[66] Therefore, it is necessary to utilize appropriate REs according to electrolyte condition. For instance, Hg/HgO is recommended to use in highly alkaline condition since it does not cause electrolyte contamination by specifically adsorbing anions.

Even though proper RE is used to measure ORR activity, RE potential could be different due to difference in natural oxidation condition of RE. Thus, a standard RE, such as reversible hydrogen electrode (RHE), is needed to compare the activity. To this end, Li *et al.* introduced a methodology in order to calibrate the RE used in the laboratory and to obtain an accurate RHE value.[25] It is performed in H_2-saturated electrolyte with Pt wires as working and counter electrodes, and the laboratory RE as the reference electrode. The potential at which the current crosses zero in the linear sweep

voltammogram becomes the thermodynamic potential for the RHE. While this procedure is most of the time not performed, it is critical to minimize the error in activity comparison.

2.2 Effect of non-faradaic processes on the number of electrons

As mentioned above, there are two ORR routes; the four-electron pathway and the two-electron pathway (Scheme 1). In order to confirm which reaction pathway dominates and to determine the overall efficiency of the electrocatalyst, the number of transferred electrons (n_e) is widely used as the parameter of choice, which can be calculated from the Levich equation. Levich equation is based on the assumption that the reduction potential is high enough and there is no diffusion barrier on the electrode surface. In some experiments, if the catalyst is not active enough (i.e. in the case of metal-free heteroatom modified carbons) the plateauing feature of limiting current is not observed. Nafion ionomer, which is frequently used for binding catalysts on the glassy carbon electrode surface, acts as a barrier that impedes diffusion of oxygen molecules to the electrode surface. Due to the above practical reasons, the Koutecky-Levich (K-L) equation is generally utilized to obtain n_e using fundamental parameters for ORR (Eq. (3)).[6,67]

$$\frac{1}{J} = \frac{1}{J_L} + \frac{1}{J_K} + \frac{1}{J_F} = \frac{1}{B\omega^{1/2}} + \frac{1}{J_K} + \frac{1}{J_F} \qquad (3)$$

where, J is the measured current density, J_L is the limiting current density, J_K is the kinetic current density, and J_F is the limiting current by diffusion through Nafion film current density. As shown in Eqs. (2) and (3), the n_e could be derived from the slope of the relation between J^{-1} and $\omega^{-1/2}$.

The reliability of the n_e from the K-L equation, however, has rarely been assessed and the parameter values are typically borrowed from literature despite differences in the experimental set-ups. Thus, investigating the practical factors affecting the error of n_e determined from the K-L equation is of practical importance. Carbon-based electrocatalysts usually have high specific surface area and they tend to have substantially high electrical double-layer capacitance and ill-defined limiting currents (Figures 3a and 3b).[40,68] When considering that there exists a maximum current density with rotating rate, geometrical area of RDE, the values of current density larger than the upper limit of oxygen reduction current density are difficult to be attributed to ORR. The most reasonable explanation for the excess reduction current is non-ORR current. There are two strategies to negate the effect of capacitive current to the final n_e; using a very slow scan rate that is lower than 1 mV s^{-1}, and subtract the non-ORR current from the total reduction current measured in the ORR test. To correct for the non-faradaic current in J, the non-ORR current obtained from CV or LSV under oxygen-depleted conditions with the same scan rate should be subtracted (Figures 3c and 3d).[42,57,58] Such approach leads to a modified K-L equation in (Eqs. (4) and (5));

$$J_{ORR} = J - J_{N_2 or\ Ar} \qquad (4)$$

$$\frac{1}{J_{ORR}} = \frac{1}{B\omega^{1/2}} + \frac{1}{J_K} + \frac{1}{J_F} \qquad (5)$$

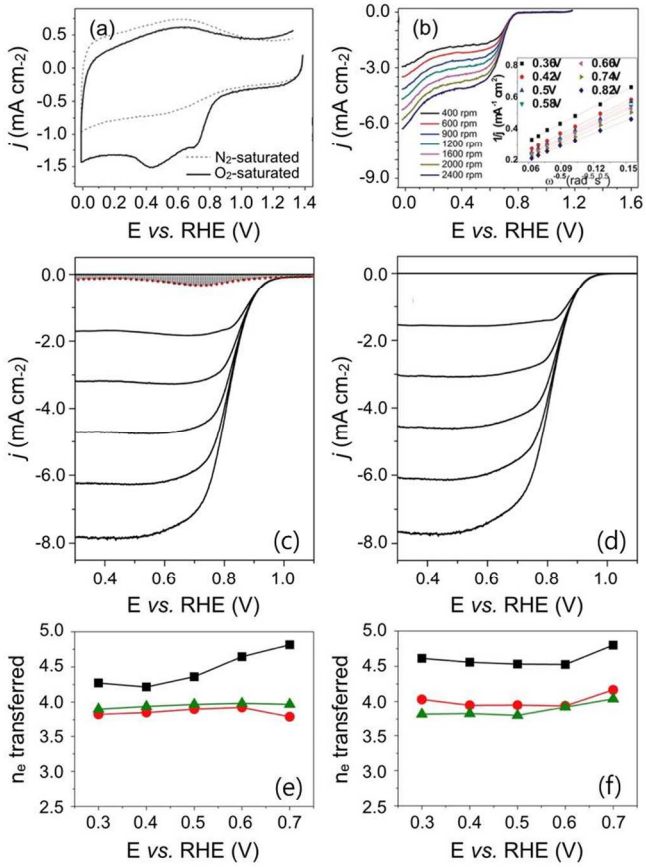

Figure 3. (a) Cyclic voltammograms (CVs) of PDMC synthesized at a pyrolysis temperature of 800 °C (PDMC-800) in O_2- and N_2-saturated 0.1 mol L^{-1} KOH solutions. (b) Polarization curves at different rotating speeds for PDMC-800 inset shows the corresponding Koutecky–Levich plots (Figure (a) and (b) were reprinted with permission from ref. 68 Copyright 2013 American Chemical Society). (c) Uncorrected LSVs using a GC RDE with 20 wt% Pt/C at different rotation rates and a scan rate of 10 mV s^{-1} in O_2-saturated 0.1 M KOH electrolyte. The shaded area indicates non-ORR current obtained at scan rate of 10 mV s^{-1} in N_2-saturated 0.1 M KOH electrolyte. (d) Corrected LSVs by subtracting non-ORR current.[57,58] The **n_e values** in (e) 20 wt% Pt/C and (f) Co-modified CNF[6] for ORR. The **n_e values** were obtained using the K-L equation for J (■), J_{ORR} (●) and the RRDE measurement (▲).[57,58]

Figures 3e and 3f demonstrate the difference in calculated n_e according to the K-L equation using the capacitive current-adjusted ORR activity and the measured ORR activity. In similar instances for Pt-based and carbon-based catalysts, n_e calculated from the measured currents are higher than the capacitance-adjusted currents. In fact, the n_e of Pt-based catalyst are unreasonably higher than the maximum value of n_e=4, while the carbon-based catalyst is close to four. On the other hand, correcting for the capacitive current leads to well-matched n_e values, when compared to the RRDE measurements. The effect of capacitive current could be understood from the fact that B slope value calculated for $J_{ORR}+J_{Ar}$ is modified by a factor of $(1+J_{Ar}/J_{ORR})^2$ to that for J_{ORR}. This subtle alteration drives the overall slope obtained from the K-L plot lower and the corresponding value of n_e higher. It means that just 3 % of the ratio of J_{Ar} to J_{ORR} can change n_e values from n_e=4 to n_e=4.2, which is big enough not to be ignored. Thus, it is recommended that researchers should consider the non-ORR component for the evaluation of dominant pathway by using n_e obtained from K-L plot fitting

results. This is crucial for preventing exaggeration in the evaluation for future works on carbon-based ORR electrocatalysts.

3. Influential factors dictating the kinetic onset potential: Scan direction

The ORR activity is evaluated through linear sweep voltammetry or cyclic voltammetry at a certain rotating rate. For some reasons, such as specifically-adsorbed anion species[69] or the initial surface state, the RDE polarization curves shows different half-wave or onset potential when using anodic or cathodic scan in most published papers. (Figure 4a and b).[21,25,28–30,67] In particular, there are some cases that used cathodic scan for developed catalyst and anodic scan for Pt/C with specific purpose (Figure 2b).[30,59] In this case, which scan direction should be chosen for representing the catalyst performance, anodic or cathodic?

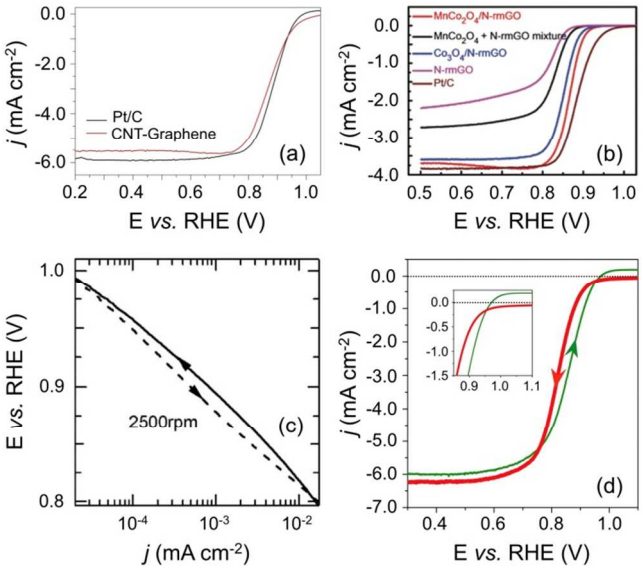

Figure 4. (a) RRDE polarization curves of Pt/C (black) and CNT–G (red) in O_2-saturated 0.1 M KOH at a rotation rate of 1,600 rpm and scan rate of 5 mV s^{-1}. Platinum data are collected from anodic sweeps (adapted by permission from Macmillan Publishers Ltd: Nature Nanotechnology (Ref.25), copyright 2012). (b) RDE voltammograms in O_2-saturated 1 M KOH at a sweep rate of 5 mV s^{-1} at 1600 rpm. The working electrode was scanned in the cathodic direction (reprinted with permission from ref. 28 Copyright 2012 American Chemical Society). (c) Tafel plot of the diffusion-corrected currents in the kinetic region of the anodic (solid) and cathodic (dashed) scans at 2500 rpm (Reprinted with permission from *J. Electrochem. Soc.*, 155, P1–P5 (2008). Copyright 2008, The Electrochemical Society). (d) LSVs using GC RDE with 20 wt% Pt/C at a scan rate of 10 mV s^{-1} and a rotating rate of 1600 rpm in O_2-saturated 0.1 M KOH electrolyte.[57,58]

In general, Pt/C catalysts usually show better onset potential in the case of positively going potential sweep (anodic) due to the oxygenated species-free surface[70] if the electrolyte does not contain highly adsorbing anion species such as phosphate or halide ions. On the contrary, it tends to have lower onset potential in the case of negatively sweep (cathodic) direction (Figure 4c and d). Although this phenomenon has been studied in Pt catalysts, it has been observed also among carbon-based catalysts.[52] In using the anodic scan direction, it is purposely done to remove oxygenated species on the catalyst surface or to minimize the side effect of other ions adsorption.[30,59] When considering the fuel cell operation condition, however, especially at the start of operation, the cathode is in the oxygen equilibrium potential due to the supply of oxygen. Therefore, cathodically (negatively) scanned linear sweeping might provide with the initial state of catalysts that reflects the real operating condition of fuel cells.[29]

As we have mentioned above, both scan directions have valid reasons for use. In the case anodic scan, it is to minimize the oxygenated species or impurities on the surface, while the cathodic scan accounts for the initial state of catalyst during the real operating condition of fuel cell. However, scan direction makes a difference in both the onset potential and diffusion limiting current, as shown in Figure 4(d). In addition, the difference in the onset potential seems to be an important factor when comparing the ORR activity among the newly developed catalysts. It is also difficult to identically define the value since the difference varies greatly depending on the catalyst. Thus, the scan direction during ORR activity measurement should be defined in order to minimize confusion and to readily compare the ORR activities. In this context, we suggest cathodically scanned linear sweeping, which might be a more proper way to measure ORR activity since all ORR catalysts will be eventually used in an actual fuel cell system.

4. Optimum electrocatalyst loading amount for minimum energy dissipation in fuel cells

During electrochemical experiments, catalyst inks derived from catalyst powders are usually used in evaluating the activity. It is well known that the microstructure of the catalyst layer, which is affected by its roughness and thickness, could be influenced by the ink composition parameters such as the amount of catalyst, kind of solvent used (e.g. ethanol, water), and the amount of ionomer (e.g. Nafion). This difference in microstructure leads to varying catalytic activity in both half-cell and actual single cell tests. [71–73] Hence, this aspect should be optimized in order to fully measure the catalytic properties. In this regard, we will investigate the effect of the catalyst ink on the ORR activity. In particular, the optimum electrocatalyst loading amount, which has been rarely discussed in carbon-based electrocatalyst literature.

Even though carbon-based catalysts have been developed through the pioneering efforts, it has yet to reach the activity and stability of Pt catalysts. In order to increase the insufficient ORR activity of carbon-based catalysts, attempts were made to use higher amounts of the catalyst than conventional Pt catalysts, considering the much lower cost of carbon relative to Pt. This has resulted in a large number of reports that measured the ORR activity using more catalyst loading to prepare the electrode (Figure 5a).[59,74,75] In addition, Pt/C reference catalyst used in literature has various Pt-carbon ratios, resulting into slightly varying activities according to the ratio used (Figure 5b).[45]

As indicated in Figures 5c and 5d, the ORR activity rises with an increasing the amount of catalyst and that the onset potential also becomes faster when the ratio of Pt to carbon is increased. In addition, this phenomenon can be equally observed in the case of carbon-based catalysts, as shown in Figure 2b.[59] Based on these results, we can conclude that the onset potential might have been positively influenced by the amount of ORR catalysts in the electrode during electrochemical cell

experiments. The observed ORR activity in the real fuel cell conditions, however, is a confluence of factors, with each factor needing to be considered carefully. As the experiment is moved from the electrochemical cell to the fuel cell, investigating the factors that affect the operation and searching the optimum amount of the catalyst is of prime importance.

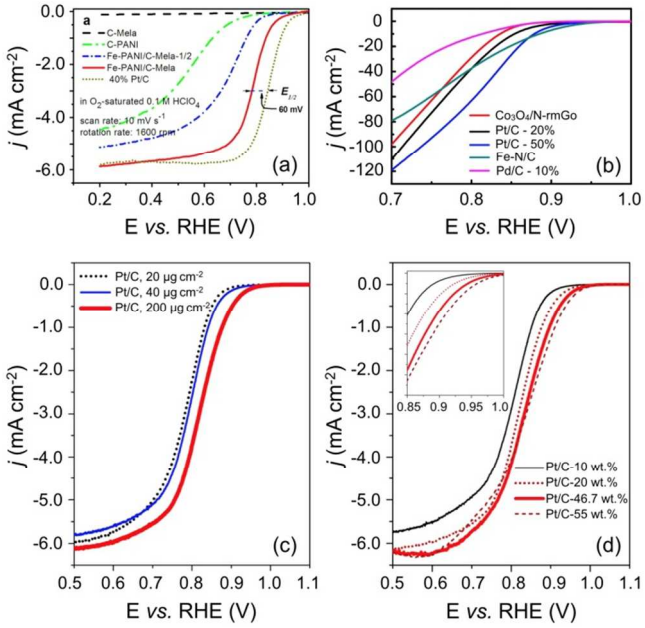

Figure 5. (a) ORR polarization plots of C-Mela, C-PANI, Fe-PANI/C-Mela-1/2, Fe-PANI/C-Mela, the catalyst loadings were fixed at 0.51 mg cm^{-2}, while the 40 wt.% Johnson Matthey (JM) Hispec 4100 Pt/C was set at 51 μgPt cm^{-2} (adapted by permission from Macmillan Publishers Ltd: Scientific Reports (Ref.71), copyright 2013). (b) Oxygen reduction polarization curves of Co_3O_4/N-rmGO, Pt/C-20%, Pt/C-50%, Fe-N/C and Pd/C-10% catalysts (catalyst loading was fixed at ~0.24 mg cm^{-2} for all samples) dispersed on carbon fiber paper (CFP) in O_2-saturated 1 M KOH electrolyte (adapted by permission from Macmillan Publishers Ltd: Scientific Reports (Ref.45), copyright 2011).[45] (c) ORR activity of 20 wt% Pt/C with different loading amount of Pt/C on glassy carbon 20 μgPt/C cm^{-2}, 40 μgPt/C cm^{-2}, and 200 μgPt/C cm^{-2}. (d) LSVs using glassy carbon rotating disk electrode with Pt/C (200 μgPt/C cm^{-2}) at a rotating rate of 1600 rpm for various wt% of Pt/C.[57,58]

As exhibited above, a loading amount that is at least five times more than Pt was applied for carbon-based electrocatalysts. This must have been done to compensate their inferior activity in comparison to Pt. Several issues, such as ohmic resistance and mass transfer limitation, however, become more pronounced during fuel cell operation when an excess loading amount of catalysts is used.

Figure 6 represents several references indicating effect of loading amount of electrocatalyst on their performances. Figure 6a is polarization plots comparing developed catalyst (Fe-PANI/C-Mela) and Pt/C.[32,57,58,74] Here, the loading amount of developed catalyst (4 mg cm^{-2}) is 20 times more than that of Pt/C (0.2 mg cm^{-2}). The developed catalyst shows even better OCV and comparable kinetic activity with Pt/C at the low current density (< 0.2 A cm^{-2}). The performance, however, is getting worse as current density is increased, indicating higher ohmic losses and mass transfer limitation losses. Figure 6b indicates polarization curves for developed catalyst (NPMC) with different loading amount of 5.3 mg cm^{-2} and 1mg cm^{-2}. The loading amount of 5.3 mg cm^{-2} shows higher kinetic activity than 1 mg cm^{-2}, which is comparable with Pt/C. On the contrary, the performance is reversed at higher current density due to higher ohmic losses of 5.3 mg cm^{-2} than that of 1 mg cm^{-2}. Figure 6c indicates polarization plots from H_2-O_2 fuel cell testing for Act-Fe-CNF (2 mg cm^{-2}, 6 mg cm^{-2}), 20 wt% Pt/C (0.5 mg cm^{-2}, 2.5 mg cm^{-2}), and 46.7 wt% Pt/C (1.0 mg cm^{-2}). Higher loading amount of Act-Fe-CNF (6 mg cm^{-2}) shows better activity than Act-Fe-CNF (2 mg cm^{-2}) at the low current density region, but it is reversed as current density is increased. It agrees well with the polarization curves in Figure 6b. The effect of loading amount on single cell performance is applied to not only carbon-based electrocatalyst but also Pt electrocatalyst. When comparing polarization curves for 20 wt% Pt/C with different loading amount of 0.5 mg cm^{-2} and 2.5 mg cm^{-2}, we found that 0.5 mg cm^{-2} shows higher power density in spite of low kinetic activity at the low current density region. However, it still shows low performance compared with 46.7 wt% Pt/C with 1.0 mg cm^{-2}.

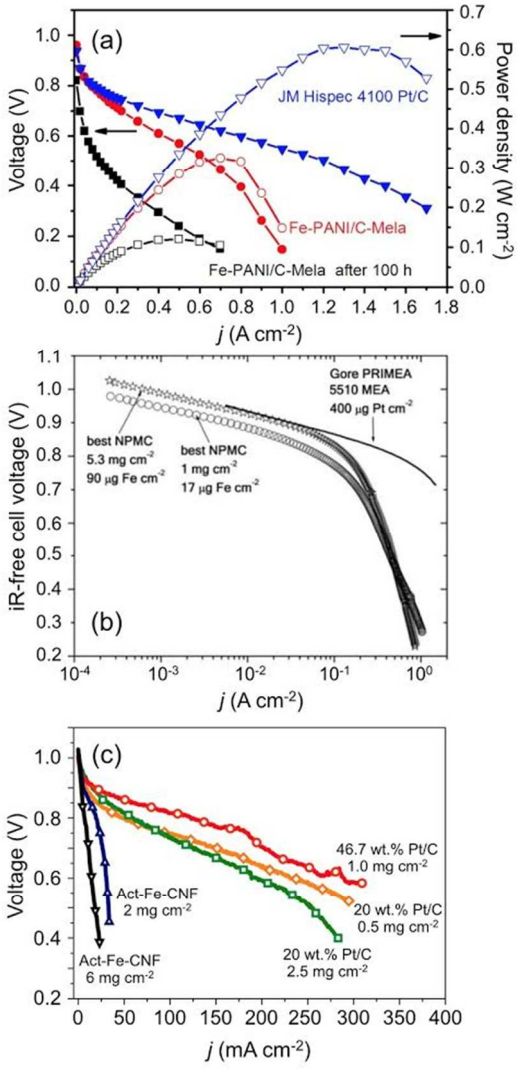

Figure 6. (a) Polarization plots of a single H_2-air PEMFC with Fe-PANI/C-Mela as the cathode (loading: 4 mg cm^{-2}), and with JM Pt/C as cathode (Pt/C loading: 0.2 mg cm^{-2}) (adapted by permission from Macmillan Publishers Ltd: Scientific Reports (Ref.71), copyright 2013). (b) Polarization curves from H_2-O_2 fuel cell testing are shown for cathodes made with the best NPMC with a loading amount of 1 mg cm^{-2}

(circles) and a loading amount of 5.3 mg cm^{-2} (stars) respectively. Also shown is a ready-to-use Gore PRIMEA 5510 membrane electrode assembly with ~0.4 mgPt cm^{-2} at cathode and anode (black line) (adapted by permission from Macmillan Publishers Ltd: Science (Ref.32), copyright 2009). (c) Polarization curves from H_2-O_2 fuel cell testing for Act-Fe-CNF (2 mg cm^{-2}, 6 mg cm^{-2}), 20 wt% Pt/C (0.5 mg cm^{-2}, 2.5 mg cm^{-2}), and 46.7 wt% Pt/C (1.0 mg cm^{-2}) in alkaline hydrogen fuel cell at 60 °C and with ambient back pressures for anode and cathode. In case of Act-Fe-CNF, 6M KOH is supplied together with hydrogen.[57,58]

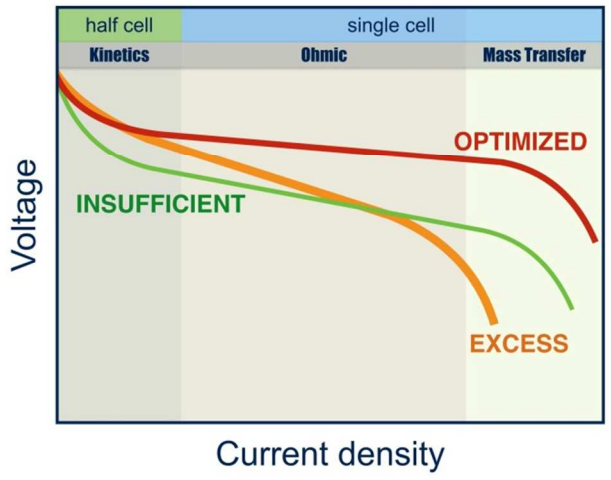

Figure 7. A schematic diagram showing the polarization curves of a cell according to three representative catalyst loading amounts (insufficient, optimized, and excess).[57,58,76]

In order to elucidate the effect of loading amount and catalytic activity on single cell performance, we provide a schematic diagram showing three representative polarization curves for insufficient, excess, and optimized catalyst amounts, as shown in Figure 7. The polarization curves can be divided into three regions: kinetics, ohmic, and mass transfer. In the kinetics region, which reflects well with the results in electrochemical cell, excess catalyst amount exhibits the best activity while insufficient catalyst amount shows the worst activity among them. It is because the amount of ORR species can be increased with increasing catalyst amount, as we have mentioned earlier. On the other hand, in ohmic and mass transfer regions, optimized catalyst amount demonstrates less energy dissipation, while the cell performances of insufficient and excess catalyst amount become worse, owing to the inappropriate thickness of catalyst layer. Hence, it is necessary to use proper catalyst amounts that do not have adverse effects in both ohmic and mass transfer regions due to inappropriate thickness if we consider practical fuel cell operation. Moreover, this also implies that the research for replacing or reducing Pt-based catalysts requires not only the development of highly active electrocatalyst but also an optimized electrode structure for the enhanced transfer of electrons or ions (conductivity), and reactant (mass transfer) to finally achieve a fuel cell performance comparable with Pt/C.

5. Concluding remarks

The promising future of non-Pt ORR electrocatalysts have encouraged many researchers to join in and explore in the development of these inexpensive ORR catalysts, as shown by the tremendous number of reports that have been published in the recent decades. Among the many alternative electrocatalysts that have been studied so far, metal-heteroatom-carbons are one of the most promising electrocatalysts in terms of comparable activity and stability to Pt/C catalysts in both electrolytes. Yet, there is still potential for further improvements by finding the identity of active sites and looking for ways to increase the number of the active sites.

In spite of numerous reports on carbon-based electrocatalysts, it is difficult to determine the state of the performance of these carbon-based ORR catalysts due to non-standardized experimental conditions to evaluate ORR performance among the developed catalysts. This situation motivates the search for ways to accurately judge the advances of carbon-based catalysts, with respect to the highly established Pt and other newly-developed catalysts. Based on both experimental observations and understanding of previous studies, we suggest that scientists and engineers developing carbon-based ORR catalysts need to consider the following:

1. The pressure and temperature should be explicitly indicated in the reports, since different oxygen concentration in electrolyte could change the diffusion limiting current. For better judgement of catalyst activity with no concern of oxygen mass transfer, it would be better to use $i_K(E)$ as the standard ORR activity, which can be derived from the K-L equation, instead of i(E) at a certain rotating rate.

2. Ag/AgCl RE should be avoided in ORR activity evaluation in alkaline solution to exclude the adverse effect of chlorine ion adsorption on the surface of catalyst and the drift of reference potential due to electrode degradation, possibly caused by the reaction between hydroxide and AgCl. Moreover, converting to RHE values would be better to readily compare the ORR activity of newly developed electrocatalysts and minimize the error in ORR activity comparison.

3. High surface area of carbon-based catalysts results into substantial non-ORR current. This non-ORR current should be subtracted from the cathodic current, in order to obtain correct number of electrons from the K-L equation with ORR-related current.

4. Even though the ORR activity on the original surface of the catalyst without any contaminants can be measured through the anodic scan, cathodic scan is recommended over the anodic scan for ORR activity measurement for matching the initial potential condition to reflect the actual operating condition in a fuel cell.

5. The ORR activity comparison with higher catalyst amount should be avoided in half-cell test because it leads to higher ohmic and mass-transfer losses in actual single cell operation. It also means that an optimum electrode structure should be developed to utilize the high amount of carbon-based electrocatalysts and electrochemical impedance spectroscopy will be useful tool for evaluating high current performance of the electrode with carbon-based catalysts.

These remarks will be helpful to evaluate the activity of ORR catalysts, especially carbon-based catalyst, in a standardized framework even though experiments are conducted in various experimental conditions.

Acknowledgements

This work was supported by Basic Science Research Program through the National Research Foundation of Korea (NRF) funded by the Ministry of Education (NRF-2013R1A1A2A10063010) and the Core Technology Development Program for Next-generation Energy Storage of Research Institute for Solar and Sustainable Energies (RISE), GIST. J. Lee is deeply indebted to the Alexander von Humboldt Foundation fellowship for experienced researchers (1141065).

Notes and references

[a] Electrochemical Reaction and Technology Laboratory (ERTL), School of Environmental Science and Engineering, GIST, Gwangju 500-712, Republic of Korea.

[b] Ertl Center for Electrochemistry and Catalysis, RISE, GIST, Gwangju 500-712, Republic of Korea. E-mail: jaeyoung@gist.ac.kr

†These authors contributed equally to this work.

Reference

1. K. Kinoshita, *Electrochemical Oxygen Technology*, Wiley, Berkeley, 1992.
2. J. Lee, B. Jeong and J. D. Ocon, *Current Applied Physics*, 2013, **13**, 309–321.
3. I. Katsounaros, S. Cherevko, A. R. Zeradjanin and K. J. J. Mayrhofer, *Angew. Chem. Int. Ed.*, 2014, **53**, 102–121.
4. D.-W. Park and J. W. Kim, *Applied Chemistry for Engineering*, 2012, **23**, 359–366.
5. J. D. Ocon, J. W. Kim, S. Uhm, B. S. Mun and J. Lee, *Phys. Chem. Chem. Phys.*, 2013, **15**, 6333–6338.
6. D. Shin, B. Jeong, B. S. Mun, H. Jeon, H.-J. Shin, J. Baik and J. Lee, *The Journal of Physical Chemistry C*, 2013, **117**, 11619–11624.
7. N. Daems, X. Sheng, I. F. J. Vankelecom and P. P. Pescarmona, *J. Mater. Chem. A*, 2014, **2**, 4085–4110.
8. G. B. Kauffman, *Chem. Educator*, 1999, **4**, 186–197.
9. A. Brouzgou, A. Podias and P. Tsiakaras, *J Appl Electrochem*, 2013, **43**, 119–136.
10. H. R. Kunz and G. A. Gruver, *J. Electrochem. Soc.*, 1975, **122**, 1279–1287.
11. U.S. Patent 4202934, 1980.
12. U.S. Patent 4447506, 1984.
13. D. Thompsett, in *Handbook of Fuel Cells*, John Wiley & Sons, Ltd, 2010.
14. S. Mukerjee and S. Srinivasan, *Journal of Electroanalytical Chemistry*, 1993, **357**, 201–224.
15. J. Zhang, F. H. B. Lima, M. H. Shao, K. Sasaki, J. X. Wang, J. Hanson and R. R. Adzic, *J Phys Chem B*, 2005, **109**, 22701–22704.
16. J. Yang, X. Chen, X. Yang and J. Y. Ying, *Energy Environ. Sci.*, 2012, **5**, 8976–8981.
17. M. K. Debe, in *Handbook of Fuel Cells*, John Wiley & Sons, Ltd, 2010.
18. L. Zhang, R. Iyyamperumal, D. F. Yancey, R. M. Crooks and G. Henkelman, *ACS Nano*, 2013, **7**, 9168–9172.
19. L. Zhang, J. Zhang, D. P. Wilkinson and H. Wang, *Journal of Power Sources*, 2006, **156**, 171–182.
20. D.-W. Wang and D. Su, *Energy Environ. Sci.*, 2014, **7**, 576–591.
21. J. Y. Cheon, T. Kim, Y. Choi, H. Y. Jeong, M. G. Kim, Y. J. Sa, J. Kim, Z. Lee, T.-H. Yang, K. Kwon, O. Terasaki, G.-G. Park, R. R. Adzic and S. H. Joo, *Scientific Reports*, 2013, **3**.
22. R. Jasinski, *Nature*, 1964, **201**, 1212–1213.
23. D. H. Jahnke, D. M. Schönborn and D. G. Zimmermann, in *Physical and Chemical Applications of Dyestuffs*, eds. F. P. Schäfer, H. Gerischer, F. Willig, H. Meier, H. Jahnke, M. Schönborn and G. Zimmermann, Springer Berlin Heidelberg, 1976, pp. 133–181.
24. S. Gupta, D. Tryk, I. Bae, W. Aldred and E. Yeager, *J Appl Electrochem*, 1989, **19**, 19–27.
25. Y. Li, W. Zhou, H. Wang, L. Xie, Y. Liang, F. Wei, J.-C. Idrobo, S. J. Pennycook and H. Dai, *Nature Nanotechnology*, 2012, **7**, 394–400.
26. S. Yang, X. Feng, X. Wang and K. Müllen, *Angewandte Chemie International Edition*, 2011, **50**, 5339–5343.
27. D. S. Su and G. Sun, *Angewandte Chemie International Edition*, 2011, **50**, 11570–11572.
28. Y. Liang, H. Wang, J. Zhou, Y. Li, J. Wang, T. Regier and H. Dai, *J. Am. Chem. Soc.*, 2012, **134**, 3517–3523.
29. B. Jeong, D. Shin, H. Jeon, J. D. Ocon, B. S. Mun, J. Baik, H.-J. Shin and J. Lee, *ChemSusChem*, 2014, **7**, 1289–1294.
30. R. Cao, R. Thapa, H. Kim, X. Xu, M. Gyu Kim, Q. Li, N. Park, M. Liu and J. Cho, *Nat Commun*, 2013, **4**.
31. D. Deng, L. Yu, X. Chen, G. Wang, L. Jin, X. Pan, J. Deng, G. Sun and X. Bao, *Angewandte Chemie International Edition*, 2013, **52**, 371–375.
32. M. Lefevre, E. Proietti, F. Jaouen and J.-P. Dodelet, *Science*, 2009, **324**, 71–74.
33. S. Uhm, B. Jeong and J. Lee, *Electrochimica Acta*, 2011, **56**, 9186–9190.
34. S. Mao, Z. Wen, T. Huang, Y. Hou and J. Chen, *Energy Environ. Sci.*, 2014, **7**, 609–616.
35. L. Ding, Q. Xin, X. Zhou, J. Qiao, H. Li and H. Wang, *J. Appl. Electrochem.*, 2013, **43**, 43–51.
36. L. Ding, J. Qiao, X. Dai, J. Zhang, J. Zhang and B. Tian, *International Journal of Hydrogen Energy*, 2012, **37**, 14103–14113.
37. L. Yang, S. Jiang, Y. Zhao, L. Zhu, S. Chen, X. Wang, Q. Wu, J. Ma, Y. Ma and Z. Hu, *Angew. Chem.*, 2011, **123**, 7270–7273.
38. L. Qu, Y. Liu, J.-B. Baek and L. Dai, *ACS Nano*, 2010, **4**, 1321–1326.
39. K. Gong, F. Du, Z. Xia, M. Durstock and L. Dai, *Science*, 2009, **323**, 760–764.
40. S. Wang, L. Zhang, Z. Xia, A. Roy, D. W. Chang, J.-B. Baek and L. Dai, *Angewandte Chemie International Edition*, 2012, **51**, 4209–4212.
41. D.-S. Yang, D. Bhattacharjya, S. Inamdar, J. Park and J.-S. Yu, *J. Am. Chem. Soc.*, 2012, **134**, 16127–16130.
42. J. Wu, Z. Yang, X. Li, Q. Sun, C. Jin, P. Strasser and R. Yang, *Journal of Materials Chemistry A*, 2013, **1**, 9889.
43. J. Liang, Y. Jiao, M. Jaroniec and S. Z. Qiao, *Angew. Chem. Int. Ed.*, 2012, **51**, 11496–11500.
44. Z. Jin, H. Nie, Z. Yang, J. Zhang, Z. Liu, X. Xu and S. Huang, *Nanoscale*, 2012, **4**, 6455–6460.
45. Y. Liang, Y. Li, H. Wang, J. Zhou, J. Wang, T. Regier and H. Dai, *Nature Materials*, 2011, **10**, 780–786.
46. R. Liu, D. Wu, X. Feng and K. Müllen, *Angewandte Chemie International Edition*, 2010, **49**, 2565–2569.
47. J. Chen, X. Wang, X. Cui, G. Yang and W. Zheng, *Chem. Commun.*, 2013, **50**, 557–559.

48. D.-S. Yang, S. Chaudhari, K. P. Rajesh and J.-S. Yu, *ChemCatChem*, 2014, **6**, 1236–1244.
49. L. Zhang and Z. Xia, *J. Phys. Chem. C*, 2011, **115**, 11170–11176.
50. D. Deng, L. Yu, X. Pan, S. Wang, X. Chen, P. Hu, L. Sun and X. Bao, *Chem. Commun.*, 2011, **47**, 10016–10018.
51. S.-F. Huang, K. Terakura, T. Ozaki, T. Ikeda, M. Boero, M. Oshima, J. Ozaki and S. Miyata, *Phys. Rev. B*, 2009, **80**, 235410.
52. A. Garsuch, A. Bonakdarpour, G. Liu, R. Yang and J. R. Dahn, in *Handbook of Fuel Cells*, John Wiley & Sons, Ltd, 2010.
53. Y. Zheng, Y. Jiao, M. Jaroniec, Y. Jin and S. Z. Qiao, *Small*, 2012, **8**, 3550–3566.
54. Z. Chen, D. Higgins, A. Yu, L. Zhang and J. Zhang, *Energy Environ. Sci.*, 2011, **4**, 3167–3192.
55. Q. Li, R. Cao, J. Cho and G. Wu, *Adv. Energy Mater.*, 2014, **4**, n/a–n/a.
56. E. Gileadi, *Physical Electrochemistry*, Wiley-VCH, Weinheim, 2011.
57. J. Lee and International Society of Electrochemistry 64th Annual Meeting, Santiago de Queretaro, Mexico, 2013.
58. J. Lee, *Ertl Center for Electrochemistry and Catalysis annual report*, 2013.
59. H. T. Chung, J. H. Won and P. Zelenay, *Nat Commun*, 2013, **4**, 1922.
60. Z. Peng, W.-Y. Yan, S.-N. Wang, S.-L. Zheng, H. Du and Y. Zhang, *Acta Physico-Chimica Sinica*, 2014, **30**, 67–74.
61. V. A. Sethuraman, J. W. Weidner, A. T. Haug, S. Motupally and L. V. Protsailo, *J. Electrochem. Soc.*, 2008, **155**, B50–B57.
62. A. Parthasarathy, S. Srinivasan, A. J. Appleby and C. R. Martin, *J. Electrochem. Soc.*, 1992, **139**, 2856–2862.
63. P. N. Ross, in *Handbook of Fuel Cells*, John Wiley & Sons, Ltd, 2010.
64. U. A. Paulus, T. J. Schmidt and H. A. Gasteiger, in *Handbook of Fuel Cells*, John Wiley & Sons, Ltd, 2010.
65. V. Stamenkovic, N. M Markovic and P. N. Ross Jr, *Journal of Electroanalytical Chemistry*, 2001, **500**, 44–51.
66. *Handbook of Reference Electrodes*, Springer, 2013.
67. T. J. Schmidt, H. A. Gasteiger, G. D. Stäb, P. M. Urban, D. M. Kolb and R. J. Behm, *J. Electrochem. Soc.*, 1998, **145**, 2354–2358.
68. R. Silva, D. Voiry, M. Chhowalla and T. Asefa, *J. Am. Chem. Soc.*, 2013, **135**, 7823–7826.
69. S. Gottesfeld, I. D. Raistrick and S. Srinivasan, *J. Electrochem. Soc.*, 1987, **134**, 1455–1462.
70. K. J. J. Mayrhofer, G. K. H. Wiberg and M. Arenz, *J. Electrochem. Soc.*, 2008, **155**, P1–P5.
71. Y. Garsany, O. A. Baturina, K. E. Swider-Lyons and S. S. Kocha, *Anal. Chem.*, 2010, **82**, 6321–6328.
72. E. Higuchi, H. Uchida and M. Watanabe, *Journal of Electroanalytical Chemistry*, 2005, **583**, 69–76.
73. W. Xing, G. Yin and J. Zhang, *Rotating Electrode Methods and Oxygen Reduction Electrocatalysts*, Elsevier, 2014.
74. H. Peng, Z. Mo, S. Liao, H. Liang, L. Yang, F. Luo, H. Song, Y. Zhong and B. Zhang, *Sci. Rep.*, 2013, **3**.
75. J.-S. Lee, G. S. Park, S. T. Kim, M. Liu and J. Cho, *Angewandte Chemie International Edition*, 2013, **52**, 1026–1030.
76. W. Vielstich, *Fuel cells: modern processes for the electrochemical production of energy*, Wiley-Interscience, 1970.

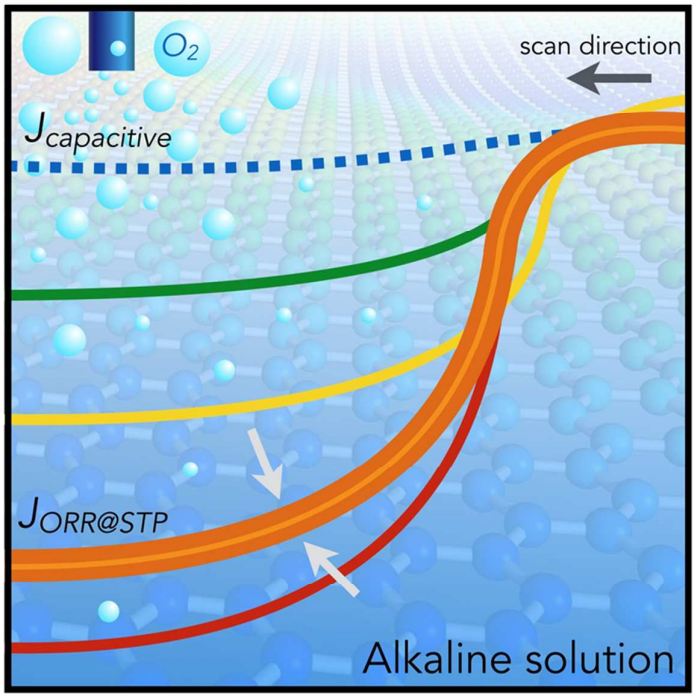

An optimal catalyst testing methodology that could allow precise benchmarking to obtain standardized ORR activity is put forward.